

Laminar flow over a small hump on a flat plate

By F. T. SMITH

Department of Mathematics, University College, London†

(Received 22 June 1972)

A boundary layer flows over a flat plate which has on it a small hump situated downstream of the leading edge. The description of the boundary-layer flow, based upon a triple-deck structure, shows how the presence of the hump generates an interaction between the inviscid region just outside the layer and the viscous region near the hump. The pressure force dominant in the boundary layer and the connexion of the local flow with the main stream develop together and are self-perpetuating, and both remain of primary significance for a wide range of hump sizes, even for a hump buried well inside the boundary layer. By consideration of the limiting cases of very small and very large humps, a consistent account of the nature of the disturbances due to the various sizes of hump is produced. The forces and couples on the hump are also evaluated.

1. Introduction

We consider high Reynolds number fluid flow past a flat plate on which there is a small excrescence, or hump. The hump is cylindrical and in cross-section has dimensions small compared with those of the boundary layer along the plate as shown in figure 1. We suppose the plate to be fixed, with a length L upstream of the hump, and choose Cartesian axes Ox^*y^* such that the leading edge is given by $x^* = -L$ and the plate is $y^* = 0$. The fluid is compressible, viscous and Newtonian, and far upstream is moving with a uniform speed U_∞^* parallel to Ox^* ; the Reynolds number is defined as $Re = U_\infty^*L/\nu_\infty^*$, where ν^* is the kinematic viscosity and the suffix ∞ denotes values far upstream. The superscript signifies dimensional quantities, and we non-dimensionalize the problem by writing the velocity components, pressure and density in the form $u^* = U_\infty^*u$, $v^* = U_\infty^*v$, $p^* = p_\infty^* + \rho_\infty^*U_\infty^{*2}p$ and $\rho^* = \rho_\infty^*\rho$. The fluid motion is assumed to be laminar and two-dimensional.

The problem has recently been considered by Hunt (1971), who used a method based on a two-region structure well inside the boundary layer and assumed that the main stream has no first-order effect on the pressure within these regions. Only very small humps of dimensional length $L\Delta$ and height $L\delta$, where

$$Re^{-\frac{1}{2}} \ll \Delta \ll Re^{-\frac{1}{4}}, \quad Re^{-\frac{1}{2}} \ll \delta \ll \Delta^{\frac{1}{2}}Re^{-\frac{1}{2}}, \quad (1.1)$$

could be accommodated in Hunt's model, as described in §8, the model being a significant first step incorporating most of the essential features of the local flow.

† Present address: Department of Mathematics, University of Southampton.

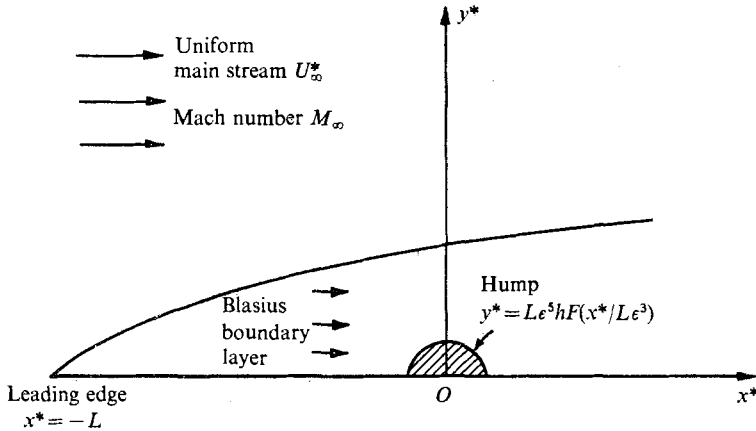


FIGURE 1. The basic problem: two-dimensional flow of a boundary layer over a small hump, of length $O(\epsilon^3 L)$ and height $O(\epsilon^5 L)$, on a flat plate, the protrusion situated at a distance L from the leading edge. The flow features for many other hump sizes can be obtained as limiting solutions of this crucial case.

In the present paper we extend the range of applicability of laminar theory to include humps of much larger size, such as those given by (1.3) below, and much smaller size (see appendix) and in the course of the analysis are able to improve upon Hunt's approach, the latter being basically correct except for the assumption mentioned above.

To analyse correctly even the effects of a hump of the size given in (1.1), and its wake, on the boundary layer flowing over it, it is our contention that the most important properties of the flow must be determined on a length scale of $O(Le^3)$, where the small parameter

$$\epsilon = Re^{-\frac{1}{3}} \tag{1.2}$$

is introduced. Accordingly we here start by examining the flow past a hump of length of $O(Le^3)$ and height of $O(Le^5)$. Specifically, we consider humps that have profiles

$$y^*/L = \epsilon^5 hF(x^*/Le^3), \tag{1.3}$$

where h is initially of order one and the function F is such that $hF(X)$ is of order one or less for all $X = x^*/Le^3$. As shown in §4, the solution for this hump provides as a special example the solution for the very small hump (1.1) as we let the larger size tend to the same order of magnitude as that given by (1.1).

The choice (1.3) is particularly convenient as the hump may then be taken as an $O(1)$ disturbance within the lower deck of a triple-deck structure. Further, the analyses in §7 and in the appendix demonstrate that the choice (1.3) is an essential one for reasons given later on in the introduction. The expansion and subsequent contraction of the boundary-layer thickness caused by the presence of the hump (1.3) produce first-order perturbations in the upper deck just outside the boundary layer that interact with and serve to maintain the lower-deck flow. The triple-deck structure, based on the matching and overall consistency of asymptotic expansions in three regions, the upper, main and lower decks, incorporates this feedback effect and we are able to satisfy the boundary conditions on the hump and those of matching upstream and outside the boundary layer.

As with previous problems studied by application of triple-deck arguments, e.g. Stewartson (1969, 1970*a, b*, 1971) and Messiter (1970), the fundamental problem for the flow over the hump reduces to that in the lower deck, where the motion is essentially viscous with an induced pressure gradient. Linearized solutions are obtained for both supersonic and subsonic main streams and the consistency of the model is demonstrated by the match achieved between these solutions and the external inviscid flow.

The special case introduced in (1.1) is solved by considering the effects of a suitably defined point disturbance within the lower deck. Similarity solutions for the decay of the velocity perturbations in the far-wake, $x^*/L\epsilon^3 \gg 1$, are found to be in agreement with the full linearized solutions, while an analysis of the near-wake of the point disturbance, $x^*/L\epsilon^3 \ll 1$, shows that the effect of the main stream remains a primary influence in the local flow. Also, this influence is independent of the subsonic or supersonic nature of the main stream. In §6, we calculate the first-order forces and couple on the general $L\epsilon^3$ by $L\epsilon^5$ hump and it is shown that the couples due to streamwise and normal stresses respectively contribute equally to the total couple C on the hump. On the other hand, the force F_2 normal to the main stream flow is zero, whilst the drag F_1 is given to first order by the undisturbed boundary-layer contribution.

In §7 we extend the description of laminar flow over small bodies by considering humps of length of order unity. Perturbation solutions of the boundary-layer equations are obtained and examination of the implied efflux from the layer shows that neglect of pressure feedback effects becomes invalid as we approach the region $x^*/L \sim \epsilon^3$. It is triple-deck theory that resolves this difficulty. The choice (1.3) is, however, even more crucial in the sense that it also enables a direct link to be made with the problem of a very small hump of dimensions $O(LRe^{-\frac{1}{2}})$ by $O(LRe^{-\frac{1}{2}})$, and this match is elucidated in the appendix. Thus a complete and self-consistent description of the wake flow is obtained for the various sizes of hump between $O(LRe^{-\frac{1}{2}})$ by $O(LRe^{-\frac{1}{2}})$ and those considered in §7 and the importance we attached to the flow problem for the hump (1.3) is justified.

The problem is of physical interest, especially with regard to the phenomenon of trip-wire transition. The aim of the present laminar theory is to provide a complete and consistent description of the flow characteristics for a wide variety of humps; ultimately an examination of, and criteria for, stability of the laminar flow would be desirable so that insight into the more realistic problems may be gained. However, it is felt that the laminar theory developed here is satisfactory as a first step in that it contains the fundamental features of the local flow problem.

2. The triple-deck structure

We here outline the systematic procedure for setting up the triple-deck appropriate to our problem. The full consistency arguments and asymptotic expansions in the three necessary regions are the same in their essential points as those laid down originally by Stewartson & Williams (1969, hereafter referred to as SW).

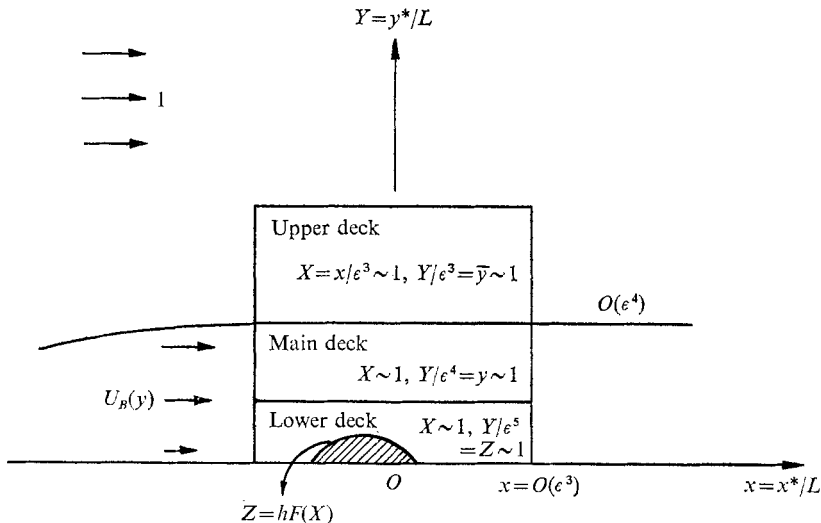


FIGURE 2. The triple-deck structure near $x^* = 0$, and the main stream and Blasius boundary-layer profiles with which the local solutions must merge. Diagram not to scale.

Starting in the *main deck* (figure 2), where $y = y^*/L\epsilon^4$ and $X = x^*/L\epsilon^3$ are the order-one co-ordinates, the flow and temperature variables are expanded as

$$\left. \begin{aligned} u &= U_B(y) + \epsilon u_1(X, y) + \epsilon^2 u_2(X, y) + \dots, \\ v &= \epsilon^2 v_1(X, y) + \epsilon^3 v_2(X, y) + \dots, \\ p &= \epsilon^2 p_2(X, y) + \epsilon^3 p_3(X, y) + \dots, \\ \rho &= R_0(y) + \epsilon \rho_1(X, y) + \dots, \\ T &= T_0(y) + \epsilon T_1(X, y) + \dots, \end{aligned} \right\} \quad (2.1)$$

where T is the absolute temperature suitably non-dimensionalized. The plate is maintained at a uniform temperature T_w , $u = U_B(y) + O(\epsilon^3)$ is the undisturbed boundary-layer profile far upstream of the hump and $R_0(y)$ the density there.

We examine whether solutions can be found that match with the known Blasius boundary layer as $X \rightarrow -\infty$ and with the main stream solutions as $y \rightarrow \infty$, and that satisfy $u = v = 0$ on the hump and on the plate. Upon substitution of (2.1) into the full Navier–Stokes equations, results (SW 3.10)–(SW 3.17) are obtained. It is then clear that only the boundary conditions upstream can be accommodated by the main-deck expansions and the flow solutions in terms of the unknown pressure force $p_2 = p_2(X)$ are

$$u_1 = A_1(X) U'_B(y), \quad v_1 = -U_B(y) A'_1(X), \quad (SW3.19)$$

together with (SW 3.24) and (SW 3.25). Here $A_1(X)$ is also unknown but we require $p_2, A_1 \rightarrow 0$ as $X \rightarrow -\infty$ and, furthermore, postulate that

$$p_2(X) \neq 0. \quad (2.2)$$

As $y \rightarrow \infty$ the match with the flow outside the boundary layer is not achieved directly by (2.1) and a further evaluation is needed in an outer region to adjust the solutions to the main stream values. The required region is the *upper deck*,

where $\bar{y} = y^*/L\epsilon^3$ and X are relevant co-ordinates, and guided by (2.1) and §4 of SW we expand

$$\begin{aligned} u &= 1 + \epsilon^2 U_2(X, \bar{y}) + \dots, \\ v &= \epsilon^2 V_2(X, \bar{y}) + \dots, \\ p &= \epsilon^2 P_2(X, \bar{y}) + \dots \end{aligned}$$

The resultant inviscid irrotational equations of motion furnish the relations

$$\left. \begin{aligned} A_1'(X) &= -\frac{1}{\pi} (1 - M_\infty^2)^{\frac{1}{2}} \int_{-\infty}^{\infty} \frac{p_2'(t) dt}{X-t} \quad (M_\infty < 1), \\ A_1(X) &= -(M_\infty^2 - 1)^{\frac{1}{2}} \int_{-\infty}^X p_2(t) dt \quad (M_\infty > 1), \end{aligned} \right\} \quad (2.3)$$

where M_∞ is the main stream Mach number; (2.3) is a matching criterion between the main and upper decks. Also, the merging with the outer flow as

$$X^2 + \bar{y}^2 \rightarrow O(\epsilon^{-3})$$

is then achieved (see also §4).

Consider now the structure of the main-deck solutions as $y \rightarrow 0$. Here again the boundary conditions cannot be satisfied directly since we assume $A_1(X) \neq 0$, from (2.2) and (2.3). A mismatch must be avoided by use of a third region, the *lower deck*, that is close to the plate and in which X and $Z = y^*/L\epsilon^5$ are the order-one co-ordinates. The perturbation to the Blasius solution is no longer small here and the expansions, implied by (2.1), (SW 5.6) and (SW 5.7), take on the forms

$$\left. \begin{aligned} u &= \epsilon U + \epsilon^2 \tilde{u}_2 + \dots, \\ v &= \epsilon^3 V + \epsilon^4 \tilde{v}_2 + \dots, \\ p &= \epsilon^2 P(X, Z) + \epsilon^3 \tilde{p}_3(X, Z) + \dots, \\ \rho &= \rho_w + \epsilon \tilde{\rho}_2 + \dots, \end{aligned} \right\} \quad (2.4)$$

where $\rho_w = R_0(0)$ is the fluid density at the plate. Purely for the sake of brevity we now set equal to unity all the order-one physical constants, e.g. $|M_\infty^2 - 1|$, involved in the affine transformations (SW 5.11) – (SW 5.16), and the Navier-Stokes equations then yield the nonlinear system

$$\left. \begin{aligned} U_X + V_Z &= 0, \\ UU_X + VU_Z &= -P'(X) + U_{ZZ}, \end{aligned} \right\} \quad (2.5)$$

with boundary conditions

$$U = V = 0 \quad \text{on} \quad Z = hF(X) \quad (\text{no-slip on the hump}), \quad (2.6)$$

$$\partial U / \partial Z \rightarrow 1 \quad \text{as} \quad X \rightarrow -\infty \quad (\text{matching with the Blasius solution } U_B(y) \sim \epsilon Z \text{ upstream}) \quad (2.7)$$

$$U \sim Z + A(X) \quad \text{as} \quad Z \rightarrow \infty \quad (\text{matching with the main deck}). \quad (2.8)$$

Here, for subsonic main stream flow,

$$A''(X) = -\frac{1}{\pi} \int_{-\infty}^{\infty} \frac{P'(t) dt}{X-t}, \quad (2.9)$$

or for the supersonic case,

$$A(X) = -\int_{-\infty}^X P(t) dt, \quad (2.10)$$

corresponding to (2.3) since $P = P(X) = p_2(X)$. In addition when $M_\infty < 1$ some limiting behaviour for $P(X)$ as $|X| \rightarrow \infty$, determined from properties in the main stream, must be satisfied; this condition is specified explicitly, and shown to be satisfied, in §4. The hump now has a profile $Z = hF(X)$ corresponding to (1.3) in dimensional terms.

In essence what this well-founded model does is to furnish via the main deck the link, between the main stream and the viscous region close to the hump, that is needed to produce the pressure force driving the flow in the latter region. This interaction between the upper and lower decks is manifested in the condition (2.8), matching the lower to the main deck, and in the relations (2.9) and (2.10), which match the main to the upper deck. It can be seen that the existence of the $\epsilon^2 P$ pressure perturbation and the interaction are mutually reinforcing.

The justification for the postulate (2.2) is the non-triviality of the solutions found in §§3–5 below, while the vanishing of any pressure term of order greater than ϵ^2 in (2.1) is necessitated by the consistency of the structure. For example, a non-zero term ϵp_1 in (2.1) implies disturbances in the main stream that could only be produced by a source existing outside the triple deck, and this disagrees with the set-up of the posed problem, the plate being flat except within the triple-deck region. Further details of the triple-deck structure are given by SW, Stewartson (1969, 1970*a, b*, 1971), Smith & Stewartson (1973) and Smith (1972) for the discussions of free interaction, corner flows, trailing-edge flows and strong blowing. The common feature of all such problems, including the present one, is a rapid change in the boundary conditions along a flat plate and their solutions all require that account be taken of the pressure-gradient effects induced by the rapid change in boundary-layer thickness ($-A(X)$) as given in (2.9) and (2.10).

For general $hF(X)$, a well-defined problem, (2.5)–(2.9) or (2.10), is set and a numerical study of the flow past the hump must be undertaken, for example by use of the methods in SW. The formulation (2.5)–(2.10) could still apply even if there is a separation bubble near the body provided that the bubble contains only relatively slowly moving fluid, for then we have effectively an extra body, given by the shape of the bubble, to consider.

3. Linearized lower-deck theory for $M_\infty < 1$

Consider now $h \ll 1$ and $M_\infty < 1$; the features for supersonic flows are explored later on in §5. Equations (2.5) may be linearized about the undisturbed boundary-layer profile by expanding the flow variables as follows:

$$U = Z + h\bar{U} + O(h^2), \quad V = h\bar{V} + O(h^2), \quad P = h\bar{P} + O(h^2), \quad A = h\bar{A} + O(h^2),$$

and if we further linearize the no-slip conditions on the hump (an alternative is to measure Z from the hump surface), we obtain

$$\bar{U}_X + \bar{V}_Z = 0, \tag{3.1}$$

$$Z\bar{U}_X + \bar{V} = -\bar{P}'(X) + \bar{U}_{ZZ} \tag{3.2}$$

to first order in h , with

$$\bar{U} = -F(X), \quad \bar{V} = 0 \quad \text{on} \quad Z = 0, \tag{3.3}$$

$$\partial \bar{U} / \partial Z \rightarrow 0 \quad \text{as } X \rightarrow -\infty, \tag{3.4}$$

$$\bar{U} \rightarrow \bar{A}(X) \quad \text{as } Z \rightarrow \infty, \tag{3.5}$$

$$\bar{A}''(X) = -\frac{1}{\pi} \int_{-\infty}^{\infty} \frac{\bar{P}'(t) dt}{X-t}. \tag{3.6}$$

Progress may be made with $F(X)$ still of general form, provided of course that $hF(X) \ll 1$ for all X . Applying Fourier transforms with respect to X to the governing equations yields the solution

$$\partial \bar{U}_f / \partial Z = B(\omega) \text{Ai}[(0+i\omega)^{\frac{1}{3}} Z],$$

where Ai is the Airy function; the other solution grows exponentially at infinity and is inadmissible because of (3.4). Here ω is the transform variable, the subscript f denotes transformed quantities and $(0+i\omega)^n$ and $(0-i\omega)^n$ are defined to be real on the negative and positive imaginary axes respectively. $B(\omega)$ is to be determined. Using conditions (3.3) and (3.5),

$$(0+i\omega)^2 \bar{U}_f(\omega, \infty) = -\frac{(0^2+\omega^2)^{\frac{1}{3}}}{0+i\omega} Q_f, \tag{3.7}$$

$$\bar{U}_f(\omega, 0) = -F_f(\omega), \tag{3.8}$$

whilst the momentum equation implies that

$$(\partial^2 \bar{U}_f / \partial Z^2)(\omega, 0) = Q_f, \tag{3.9}$$

where $Q \equiv d\bar{P}/dX$. Hence

$$\bar{U}_f = B(\omega) \int_0^Z \text{Ai}[(0+i\omega)^{\frac{1}{3}} t] dt - F_f(\omega),$$

and using (3.7) and (3.9) we are able to solve for Q_f and $B(\omega)$. Upon inverting the transforms the pressure gradient and effective skin friction $\tau = 1 + h\bar{U}_Z(X, 0)$ are given in terms of integrals in the complex- ω plane involving $F_f(\omega)$. Formally both results may then be expressed, after some manipulation, in real convolution form and give solutions for the flow ahead of and over the hump, and in the wake immediately downstream, as follows:

$$\frac{dP}{dX} = \frac{h\theta^3}{2\pi} \int_{-\infty}^{\infty} F(X-t) \alpha(t) dt, \tag{3.10}$$

$$\tau = 1 - \frac{3h \text{Ai}(0) \theta^{\frac{2}{3}}}{2\pi} \int_{-\infty}^{\infty} F(X-t) \beta(t) dt, \tag{3.11}$$

where

$$\alpha = \left\{ \begin{array}{l} \int_0^{\infty} \frac{s^2(3^{\frac{1}{3}}s^{\frac{1}{3}}-2)e^{-\theta st} ds}{1-3^{\frac{1}{3}}s^{\frac{1}{3}}+s^{\frac{2}{3}}}, \\ 2 \int_0^{\infty} \frac{s^2 e^{\theta st} ds}{1+s^{\frac{2}{3}}}, \end{array} \right. \quad \beta = \left\{ \begin{array}{l} \int_0^{\infty} \frac{s^{\frac{2}{3}}(3^{\frac{1}{3}}s^{\frac{1}{3}}-1)e^{-\theta st} ds}{1-3^{\frac{1}{3}}s^{\frac{1}{3}}+s^{\frac{2}{3}}} \quad (t > 0), \\ 2 \int_0^{\infty} \frac{s^{\frac{2}{3}} e^{\theta st} ds}{1+s^{\frac{2}{3}}} \quad (t < 0), \end{array} \right\} \tag{3.12}$$

and we have introduced the number $\theta = [-3 \text{Ai}'(0)]^{\frac{3}{2}} = 0.8272\dots$. The different forms of solution for $t < 0$ and $t > 0$ correspond to closing the contour in $\text{Im } \omega < 0$ and $\text{Im } \omega > 0$ respectively.

For any well-behaved hump profile $hF(X)$ we thus have the distribution of pressure gradient $P'(X)$ and skin friction $\tau(X)$ to first order in h for all values of X . An example is given in figure 3 below.

4. Application to very small humps

We shall now discuss a special case. In order to deal with the flow problem for a very small hump, for example, one of dimensions $L\Delta$ by $L\delta$, where $\Delta \ll \epsilon^4$ and $\delta \ll \Delta^{1/2}\epsilon^4$ (see (1.1) and, for clarification of the scalings, §8), it is necessary for our present hump to tend to a point disturbance at the origin on the ϵ^3 scale in x^*/L . Let us therefore consider a hump with maximum height of order $Lh\epsilon^5/\lambda$, length of $O(L\epsilon^3\lambda)$, satisfying $\int_{-\infty}^{\infty} F(X) dX = 1$ and therefore becoming a delta function within the lower deck as $\lambda \rightarrow 0$. Concrete examples are

$$\left. \begin{aligned} F(X) &= \frac{3}{4}(1/\lambda - X^2/\lambda^3) \\ F(X) &= 1/2\lambda \end{aligned} \right\} \text{for } |X| < \lambda, \text{ zero otherwise.} \tag{4.1}$$

The analysis below applies directly, however, to any shape of hump with length and height of these orders. If we keep $h/\lambda \ll 1$, the fluid motion generated by the presence of such a hump still lies within the scope of the above linearized analysis for all λ —provided also that $\lambda \rightarrow 0$ is defined suitably and we remain outside the $L\epsilon^6$ by $L\epsilon^6$ region, as explained below.

Letting $\lambda \rightarrow 0$, but with $h/\lambda \rightarrow 0$ also, we obtain

$$F_f(\omega) = \int_{-\infty}^{\infty} F(X) dX = 1,$$

which is independent of ω , and from (3.10) and (3.11) therefore

$$\frac{dP}{dX} = \frac{h\theta^3}{2\pi} \int_0^{\infty} \frac{s^2 e^{-\theta X s} (3^{1/2} s^{3/4} - 2) ds}{1 - 3^{1/2} s^{3/4} + s^{3/2}}, \tag{4.2}$$

$$\tau(X) = 1 - \frac{3h \text{Ai}(0) \theta^{3/4}}{2\pi} \int_0^{\infty} \frac{s^{3/4} e^{-\theta X s} (3^{1/2} s^{3/4} - 1) ds}{1 - 3^{1/2} s^{3/4} + s^{3/2}}, \tag{4.3}$$

for $X > 0$, that is, everywhere in the wake of the hump. Similar expressions may be obtained from (3.12) for the pressure gradient and skin friction in $X < 0$ (see figure 4), showing how the presence of the hump is anticipated far ahead of the actual location of the hump. We also include for use below the solution for the displacement thickness $\bar{A}(X)$ obtained via (3.6); by operations similar to those above it is found that

$$\bar{U}(X, \infty) = \bar{A}(X) = -\frac{\theta}{2\pi} \int_0^{\infty} \frac{e^{-\theta X t} t^{3/4} dt}{1 - 3^{1/2} t^{3/4} + t^{3/2}} \text{ for } X > 0. \tag{4.4}$$

Now we wish in particular to ascertain the flow characteristics for the hump described in (1.1), and in our present terms this corresponds to taking the limits $\lambda \rightarrow 0, h \rightarrow 0, h/\lambda \rightarrow 0$ such that $h/\lambda \sim \delta/\epsilon^5$ (so that the height is of the order of magnitude required by (1.1)) and $\lambda\epsilon^3 \sim \Delta$ (equating the order of the length to that in (1.1)); this of course is the only true sense in which any of the asymptotic analysis here can be considered valid. Hence

$$h \sim \Delta\delta/\epsilon^8 (\ll 1), \quad \lambda \sim \Delta/\epsilon^3 (\gg h) \tag{4.5}$$

are the relevant limits.

For $X \ll 1$, equation (4.2) shows that

$$P'(X) \sim (3^{\frac{1}{2}}h/2\pi)\theta^{\frac{1}{3}}\Gamma(\frac{5}{3})X^{-\frac{5}{3}} + \dots \tag{4.6a}$$

and so, as $X \rightarrow O(\lambda)$, i.e. remaining close to the hump (on the Le^3 scale) as we let the hump shrink, a pressure gradient of order $\delta/\Delta^{\frac{2}{3}}\epsilon^4$ is implied for the local flow, taking into account the scaling factors for P and X . Similarly, inspection of the integral in (4.3) shows an $X^{-\frac{5}{3}}$ behaviour for small X , which implies a skin-friction perturbation of order $\delta/\Delta^{\frac{1}{3}}\epsilon^8$ when the limits in (4.5) are taken, with X remaining of $O(\lambda)$. Also from (4.4) we find

$$A(X) \sim -\frac{h\theta}{2\pi} \left(\frac{3^{\frac{1}{2}}\pi}{2} - 3(\theta X)^{\frac{1}{3}}\Gamma(\frac{2}{3}) + \dots \right) \text{ as } X \rightarrow 0. \tag{4.6b}$$

We return to these results, describing the immediate neighbourhood downstream of this point disturbance, in §8.

Considering the general point disturbance again, the complete and efficient rational basis on which the triple-deck structure is built allows the results of (4.2)–(4.4) to be applied directly not only to the $L\Delta$ by $L\delta$ hump but also to the whole range of heights given by $\epsilon \ll h/\lambda \ll 1$. Thus for all such values of h/λ the triple-deck structure still applies downstream, where the flow due to the hump is a small perturbation of the Blasius solution, and for general body shape $F(X)$, provided $hF(X)$ is well-behaved, separation of the flow will not occur according to (4.3). Indeed, as the hump shrinks the wake solutions we have obtained finally fail, and a basically different character for the flow arises, only when the limit $h/\lambda \sim \epsilon$ is reached. At that stage ($\lambda \sim \epsilon^3$, $h \sim \epsilon^4$), the triple-deck solution predicts a pressure of $O(\epsilon^4)$ and a skin-friction perturbation that overtakes the Blasius shear contribution about which we originally linearized, and the necessary re-evaluation of the local flow shows that the full Navier–Stokes equations including a pressure force $p(x^*/Le^6, y^*/Le^6)$ are relevant in the region Le^6 by Le^6 . This hierarchy of regions is analogous to that for the trailing-edge problem discussed in Stewartson (1969) and Messiter (1970), and in the appendix we show that there is a *direct* match between the wake solutions for the Le^6 by Le^6 hump and those for the hump (1.3) that we initially considered. Thus, outside this very small region the main features occur on the Le^3 by Le^3 scale, the main stream influence remains a dominant effect and the first-order flow is as described above. The analysis below, and in §§5 and 6, for a point disturbance therefore holds true for all humps of the above description including that of (1.1).

We now obtain the flow solutions in the wake far downstream of the point disturbance ($X \gg 1$). The results are easily extended to the problem of a body of length of $O(Le^3\lambda)$ and height of $O(Le^5h/\lambda)$, with λ finite, by inclusion of a factor

$$\int_{-\lambda}^{\lambda} F(X) dX$$

throughout since for $X \gg 1$ this body is effectively a point disturbance also, from (3.10) and (3.11). Examining (4.2)–(4.4), we have for $X \gg 1$

$$dP/dX = -2h/\pi X^3 + \dots, \tag{4.7}$$

$$\tau(X) = 1 + (3h \text{Ai}(0)/2\pi\theta^{\frac{1}{3}})\Gamma(\frac{2}{3})X^{-\frac{2}{3}} + \dots, \tag{4.8}$$

$$A(X) = - (h\Gamma(\frac{7}{3})/2\pi\theta^{\frac{1}{3}})X^{-\frac{7}{3}} + \dots \tag{4.9}$$

Equation (4.8) shows that the skin friction returns to the Blasius value as we proceed downstream out of the lower deck, whilst the decay of (4.7) agrees with the matching requirement on the pressure obtained from the external flow region. For there y^*/L and x^*/L are of $O(1)$ and the perturbation velocity potential ϕ satisfies $\nabla^2\phi = 0$ with $\phi_Y = h\epsilon^2 dF_1/dx$ on $Y = 0$ (from linearized thin-wing theory), where $F_1(x) \equiv F(X)$, $Y = y^*/L$ and $x = x^*/L$. Hence the pressure along $Y = 0$ produced by the external inviscid theory is

$$p_{\text{ext}} = \frac{\epsilon^2 h}{\pi} \int_{-\infty}^{\infty} \frac{F_1'(t) dt}{t-x} = \frac{\epsilon^2 h}{\pi} \int_{-\infty}^{\infty} \frac{F'(s) ds}{s-X}$$

upon substituting $t = \epsilon^3 s$ and $X = x/\epsilon^3$. As we let $F(t)$ become the delta function we obtain $p_{\text{ext}}/\epsilon^2 = h/\pi X^2$ in the limit, using properties of the delta function. This matches with (4.7) as $X \rightarrow \infty$, showing that the required consistency is obtained by the triple-deck model. Similarly, it can be shown that the solution for dP/dX when X is negative, using (3.12), agrees with the solution for dp_{ext}/dx as $X \rightarrow -\infty$ and $x \rightarrow 0^-$ respectively. Matching of $P_2(X, \bar{y})$ in the upper deck is likewise verified, and hence we see that even the point disturbance generates a major effect just outside the main part of the boundary layer.

The known pressure-gradient expansion (4.7) enables the solutions for U and V for large X to be found to first order in h in similarity form. With the similarity variable $\eta = Z/X^{3/4}$, \bar{U} must be written as

$$\bar{U} = X^{-3/4} G'(\eta) + \dots \quad \text{for } X \rightarrow \infty \tag{4.10}$$

to comply with the boundary condition $\bar{U} \rightarrow \bar{A}(X)$ as $Z \rightarrow \infty$, where $A(X)$ is given by (4.9) for $X \gg 1$. Substituting (4.10) and the corresponding form

$$\bar{V} = (2G + \frac{1}{3}\eta G') X^{-3/4} + \dots \tag{4.11}$$

into the equation of motion (3.2) and retaining the highest order terms produces the following equation, with a prime denoting $d/d\eta$:

$$G''' + \frac{1}{3}\eta^2 G'' + 2\eta G' = 2G = -2/\pi \tag{4.12}$$

which is to satisfy the boundary condition $G(0) = G'(0) = 0$ (no slip at the wall) and

$$G'(\infty) = -\Gamma(\frac{7}{3})/2\pi\theta^{3/4} \tag{4.13}$$

(matching as $Z \rightarrow \infty$ with X large but fixed). An important point here is that the pressure gradient still has an effect on the first-order flow for large X , via the right-hand side of (4.12).

The general solution for $G(\eta)$ may be obtained by the (standard) procedure of writing $G = \eta H(\eta)$ and solving for $dH/d\eta$ and we find that

$$G = \frac{1}{\pi} + C\eta + A\eta \int_0^\eta e^{-s_1} (15 - \eta_1^3) d\eta_1 + B\eta \int_\infty^\eta \text{P} \int_0^\infty \frac{e^{-rs_1}}{r-1} (\frac{5}{3}r^{3/2} - sr^{3/2}) dr d\eta_1,$$

with $s_1 = \frac{1}{9}\eta_1^3$ and P denoting a Cauchy principal value. The wall boundary conditions then produce

$$B = 1/3^{3/4}\pi\Gamma(\frac{2}{3}), \quad C = -4B\Gamma(\frac{1}{3})\pi/3^{1/4},$$

whilst from (4.13), $C + 12A\Gamma(\frac{1}{3})3^{-1/4} = -\frac{4}{9}\Gamma(\frac{1}{3})/2\pi\theta^{3/4}$.

With A, B and C thus determined, we may evaluate

$$G''(0) = 30A + \frac{10}{3}B\pi/3^{\frac{1}{2}} = \frac{5}{9}3^{\frac{1}{2}}/\pi\theta^{\frac{1}{2}}. \tag{4.14}$$

Hence from (4.10) we have

$$\tau(X) = 1 + h[X^{-\frac{5}{2}} \times \frac{5}{9}3^{\frac{1}{2}}/\pi\theta^{\frac{1}{2}} + \dots] + O(h^2) \quad \text{for } X \gg 1,$$

agreeing with the already calculated expansion (4.8) for the skin friction.

The flow pattern far downstream of the hump is therefore established. As $X \rightarrow \infty$ the perturbations produced by the point disturbance decay and the flow reverts to the Blasius form. The streamwise velocity perturbation behaves like $Z/X^{\frac{3}{2}}$ for small Z and like $X^{-\frac{7}{2}}$ for $\eta \rightarrow \infty$, the pressure decays like X^{-2} and matches with the external inviscid solution. The flow to first order retains both the $Z + A(X)$ interaction character for $Z \rightarrow \infty$ and the pressure-gradient effect. The results for a point disturbance are also obtainable by use of the representations in (4.1) and the convolution expressions in (3.10) and (3.11) and by letting $\lambda \rightarrow 0$ in the resulting exact solutions. The parabolic hump in (4.1) is clearly more satisfactory in this respect as use of the step function entails extra consideration of the flow near the corners of the hump. However, the delta function analysis only is included because of its greater simplicity.

5. Supersonic main stream

For $M_\infty > 1$ the lower-deck problem for the hump of general shape $Z = hF(X)$, where $h \ll 1$, is in many respects like that for the subsonic problem of §5. Linearization produces equations (3.1)–(3.5) but with

$$\bar{A}(X) = - \int_{-\infty}^X \bar{P}(t) dt, \tag{5.1}$$

instead of (3.6). Hence

$$\bar{U}_f(\omega, \infty) = -\bar{P}_f(0 + i\omega)^{-1} \quad \text{and} \quad (\partial^2 \bar{U}_f / \partial Z^2)(\omega, 0) = \bar{P}_f(0 + i\omega)$$

replace (3.7) and (3.9) respectively and we find that

$$B(\omega) = \frac{3F_f(\omega)(0 + i\omega)^{\frac{3}{2}}}{(0 + i\omega)^{\frac{3}{2}} - \theta^{\frac{1}{2}}}, \quad \bar{P}_f = \frac{-\theta^{\frac{1}{2}}(0 + i\omega)F_f(\omega)}{(\theta + i\omega)^{\frac{1}{2}} - \theta^{\frac{1}{2}}}. \tag{5.2), (5.3)}$$

Thence, by contour integration much akin to that for §3 but not so complicated, formally

$$\left. \begin{aligned} P(X) &= -\frac{h\theta^2}{2\pi} \int_{-\infty}^{\infty} F(X-t)R(t) dt, \\ \tau(X) &= 1 - \frac{3^{\frac{3}{2}}h \text{Ai}(0)}{2\pi} \theta^{\frac{1}{2}} \int_{-\infty}^{\infty} F(X-t)S(t) dt, \end{aligned} \right\} \tag{5.4}$$

where

$$R(t) = \begin{cases} 3^{\frac{1}{2}} \int_0^{\infty} \frac{s^{\frac{1}{2}} e^{-\theta st} ds}{1 + s^{\frac{1}{2}} + s^{\frac{3}{2}}}, & S(t) = \begin{cases} \int_0^{\infty} \frac{s^{\frac{1}{2}}(1 + s^{\frac{1}{2}}) e^{-\theta st} ds}{1 + s^{\frac{1}{2}} + s^{\frac{3}{2}}} & \text{for } t > 0, \\ \frac{1}{2} 3^{\frac{1}{2}} \pi e^{\theta t} & \text{for } t < 0. \end{cases} \end{cases}$$

For any point disturbance at the origin as defined in §4 we therefore have the wake solutions

$$P(X) = \frac{-3^{\frac{1}{2}} h \theta^2}{2\pi} \int_0^\infty \frac{s^{\frac{2}{3}} e^{-\theta X s} ds}{1 + s^{\frac{4}{3}} + s^{\frac{5}{3}}}, \tag{5.5}$$

$$\tau(X) = 1 - \frac{3^{\frac{2}{3}}}{2\pi} h Ai(0) \theta^{\frac{2}{3}} \int_0^\infty \frac{s^{\frac{5}{3}} (1 + s^{\frac{4}{3}}) e^{-\theta X s} ds}{1 + s^{\frac{4}{3}} + s^{\frac{5}{3}}} \tag{5.6}$$

to first order in h . These give exactly the same $X^{-\frac{5}{3}}$ and $X^{-\frac{4}{3}}$ behaviour for the pressure gradient and skin friction respectively near $X = 0$ as those worked out for the subsonic flow, equation (4.6) ff., and from (5.1) the displacement function $A(X)$ has the same form as (4.6). So the comments in the previous section on the application of the triple-deck results to the very small hump problem as $X \rightarrow O(\lambda)$ also apply wholesale to supersonic flows. Likewise, the flow ahead of the hump is easily determined from (5.4) and we observe that $A(X)$ is continuous and non-zero at $X = 0$. Graphs for $M_\infty > 1$ are included in figure 4.

Concerning the wake far downstream of the point disturbance, (5.5) and (5.6) yield

$$\left. \begin{aligned} P(X) &= - (3^{\frac{1}{2}} h / 2\pi \theta^{\frac{2}{3}}) \Gamma(\frac{1}{3}) X^{-\frac{5}{3}} + \dots, \\ \tau(X) &= 1 - (3^{\frac{2}{3}} h / 2\pi) Ai(0) \Gamma(\frac{2}{3}) X^{-\frac{4}{3}} + \dots, \\ A(X) &= - (2 \times 3^{\frac{1}{2}} h / 9\pi \theta^{\frac{2}{3}}) \Gamma(\frac{1}{3}) X^{-\frac{2}{3}} + \dots \end{aligned} \right\} \tag{5.7}$$

as $X \rightarrow \infty$. The last two expressions are similar to (4.8) and (4.9) but now the skin-friction perturbation is negative. The approach of the far-wake flow to the upstream Blasius solution is therefore of the same form as that for $M_\infty < 1$, the first-order velocity perturbations \bar{U} and \bar{V} having the similarity forms (4.10) and (4.11) respectively. However, the pressure here decays faster than the X^{-2} decay of the $M_\infty < 1$ case and hence the governing equation is

$$G''' + \frac{1}{3} \eta^2 G'' + 2\eta G' - 2G = 0,$$

the pressure effect in the far wake being absent to first order. The solution satisfying the wall conditions $G(0) = G'(0) = 0$ is

$$G = A\eta \int_0^\eta e^{-s_1(15 - \eta_1^3)} d\eta_1$$

whilst matching \bar{U} with $h^{-1}A(X)$ as given in (5.7) implies that

$$G'(\infty) = -2 \times 3^{\frac{1}{2}} \Gamma(\frac{1}{3}) / 9\pi \theta^{\frac{2}{3}}.$$

Hence $A = -1/2\pi \theta^{\frac{2}{3}} 3^{\frac{1}{3}}$ and $G''(0) = -5/\pi \theta^{\frac{2}{3}} 3^{\frac{2}{3}}$. The skin friction implied by the similarity solutions therefore agrees with that in (5.7) and overall the decay of the velocity perturbations in the far wake has the same character as that in the subsonic case. Because of the close similarity between the results for all X whether the main stream be subsonic or supersonic (see also figure 3), the remaining sections dealing with the hump problem apply equally well to both the $M_\infty < 1$ and the $M_\infty > 1$ regimes.

6. Forces and couple on the hump

We now examine the forces and couple acting on a hump of general shape:

$$Z = hF(X) \quad \text{where} \quad h \ll 1, \quad (6.1)$$

and suppose the hump to have length $2\lambda\epsilon^3L$, with λ finite at present. To make comparisons between the contributions to the total force from the different stress components acting at the body/fluid interface, we first relate all the terms involved to the $O(1)$ co-ordinates $x = x^*/L$ and $Y = y^*/L$ and to the unscaled variables $u = u^*/U_\infty^*$, $v = v^*/U_\infty^*$ and $p = (p^* - p_\infty^*)/\rho_\infty^* U_\infty^{*2}$. By considering the stresses on an element ds of the hump surface, the streamwise force F_1 acting on the whole body is then found to be

$$F_1 = \int (p(x) \sin \alpha ds + \tau_{xx} dY + \tau_{xY} dx),$$

where $\alpha = \tan^{-1}(dY/dx)$, $\tau_{xx} = 2\epsilon^6 u_x$ and $\tau_{xY} = \epsilon^8(u_Y + v_x)$.

Written in terms of the lower-deck variables of (2.4) ff., we therefore have

$$F_1 = \int_{-\lambda}^{\lambda} [\epsilon^7 h^2 \bar{P} \bar{F}'(X) + 2\epsilon^{11} h^2 \bar{U}_X|_{Z=0} F'(X) + \epsilon^7 (1 + h\bar{U}_Z|_{Z=0} + h\epsilon^4 \bar{V}_X|_{Z=0})] dX,$$

where linearization is applied at $Z = hF(X)$. Hence the highest order term remains the Blasius-shear contribution, which gives

$$F_1 = 2\lambda\epsilon^7. \quad (6.2)$$

Likewise the force acting on the body in the Y direction is given by

$$F_2 = \int_{-\lambda}^{\lambda} [-\epsilon^5 h \bar{P} + 2\epsilon^{11} h \bar{V}_Z|_{Z=0} + \epsilon^9 h (1 + h\bar{U}_Z|_{Z=0} + h\epsilon^4 \bar{V}_X|_{Z=0}) F'(X)] dX.$$

Upon integration, the Blasius-shear contribution gives a zero net force, so that

$$F_2 = 0 \quad \text{to} \quad O(\epsilon h^2). \quad (6.3)$$

The clockwise couple on the hump due to streamwise stresses only (i.e. due to force elements dF_1) is, by similar reasoning,

$$C_1 = \int_{-\lambda}^{\lambda} [\epsilon^7 h^2 \bar{P} F'(X) + 2\epsilon^{11} h^2 \bar{U}_X|_{Z=0} F'(X) + \epsilon^7 (1 + h\bar{U}_Z|_{Z=0} + h\epsilon^4 \bar{V}_X|_{Z=0}) \times h\epsilon^5 F(X)] dX,$$

of which the highest order term gives

$$C_1 = \epsilon^{12} h \int_{-\lambda}^{\lambda} F(X) dX. \quad (6.4)$$

The couple due to stresses normal to the main stream is

$$C_2 = \int_{-\lambda}^{\lambda} [-\epsilon^5 h \bar{P} + 2\epsilon^{11} h \bar{V}_Z|_{Z=0} + \epsilon^9 h (1 + h\bar{U}_Z|_{Z=0} + h\epsilon^4 \bar{V}_X|_{Z=0}) F'(X)] \times -\epsilon^3 X dX,$$

so that to first order in h

$$\begin{aligned} C_2 &= -\epsilon^{12} h \int_{-\lambda}^{\lambda} F'(X) X dX \\ &= \epsilon^{12} h \int_{-\lambda}^{\lambda} F(X) dX. \end{aligned} \quad (6.5)$$

Therefore the total couple on the hump is given to first order in h by

$$C = 2Re^{-\frac{3}{2}h} \int_{-\lambda}^{\lambda} F(X) dX,$$

a result holding true for any body of the form (6.1), and for both supersonic and subsonic main stream flows. The contributions to C from C_1 and C_2 are equal in magnitude and sense, both being clockwise-positive. In particular, applying the result to the case of a point disturbance (of any shape; for example, those of (4.1)) within the lower deck and letting $\lambda \rightarrow 0$, we therefore obtain

$$C_1 = C_2 = \frac{1}{2}C = Re^{-\frac{3}{2}h}$$

to first order in h and ϵ , for any very small hump. For the $L\Delta$ by $L\delta$ examples defined in (1.1) and using (4.5), this suggests that

$$C_1 = C_2 = \frac{1}{2}C = \Delta\delta Re^{-\frac{1}{2}}. \tag{6.6}$$

7. Longer humps and the implications of boundary-layer theory

In order to be systematic in dealing with the small-hump problems, we show here that the triple-deck structure, describing the flow past the humps of §§2-6, is implied by the breakdown of the boundary-layer theory given below that deals with humps of length greater than $O(L\epsilon^3)$.

For such long humps the following analysis shows that there is no first-order pressure-gradient effect in the flow over the majority of the hump and its wake if the hump is taken to be of height $HL\epsilon^4$, where $1 \gg H \gg \epsilon^4$ (or $H = \epsilon h$). Consider the hump profile

$$y^* = HL\epsilon^4 f(x^*/L), \tag{7.1}$$

where L is as in figure 1 and $f(x^*/L)$ is of $O(1)$ or less for all $x^* > 0$. We assume that the hump produces no $O(H)$ effect in the main stream, the major effects due to the introduction of the hump being confined to the boundary layer flowing past. The assumption is investigated *a posteriori*.

Scaling $y = y^*/L\epsilon^4$ and $x = x^*/L$, so that the hump becomes $y = Hf(x)$, we expand

$$\left. \begin{aligned} u &= [U_B(x, y) + Hu_1(x, y) + \dots], \\ v &= \epsilon^4 [V_B(x, y) + Hv_1(x, y) + \dots], \\ p &= [Hp_1(x, y) + \dots], \end{aligned} \right\} \tag{7.2}$$

terms of order H^2 and ϵ^4 and smaller being omitted in the square brackets. Here $U_B(x, y)$ is the Blasius flat-plate solution given by $U_B = f'_B(\eta)$, where now $\eta = y/[2(1+x)]^{\frac{1}{2}}$, since the leading edge is situated at $x = -1$, and a prime denotes $d/d\eta$. The full Navier-Stokes equations then yield the following.

$$\text{Continuity:} \quad (U_{Bx} + Hu_{1x} + \dots) + (V_{By} + Hv_{1y} + \dots) = 0, \tag{7.3}$$

x momentum:

$$\begin{aligned} (U_B + Hu_1 + \dots)(U_{Bx} + Hu_{1x} + \dots) + (V_B + Hv_1 + \dots)(U_{By} + Hu_{1y} + \dots) \\ = -(Hp_{1x} + \dots) + (U_{Byy} + Hu_{1yy} + \dots), \end{aligned} \tag{7.4}$$

y momentum:

$$p_1 = p_1(x).$$

Since we hypothesize no $O(H)$ effects as $y \rightarrow \infty$,

$$p_1 = 0. \tag{7.5}$$

Examining (7.3) and (7.4), we see that the *combined velocity*

$$(U = U_B + Hu_1, V = V_B + Hv_1)$$

satisfies to $O(H)$ the flat-plate boundary-layer equations

$$U_x + V_y = 0, \quad UU_x + VU_y = U_{yy}, \tag{7.6}$$

together with

$$\begin{aligned} U = V = 0 & \quad \text{on } y = Hf(x), \\ U \rightarrow 1 & \quad \text{as } y \rightarrow \infty, \\ U = U_B(0, y) = f'_B(y) & \quad \text{at } x = 0. \end{aligned}$$

The second condition here is that we require $u = 1 + o(H)$ outside the boundary layer.

The solution for U and V follows by transforming to the variables

$$y_1 = y - Hf(x), \quad V_1 = V - HUdf/dx.$$

For then, with y_1 replacing y , (U, V_1) satisfies (7.6) and the boundary conditions become flat-plate ones with initial profile $U_B(0, y_1)$, since $f(0) = 0$, and $U \rightarrow 1$ as $y_1 \rightarrow \infty$. Hence

$$U = U_B(x, y_1), \quad V_1 = V_B(x, y_1),$$

where now

$$U_B(x, y_1) = f'_B(\eta_1), \quad V_B(x, y_1) = (\eta_1 f'_B - f_B) / [2(1+x)]^{1/2}, \quad \eta_1 = y_1 / [2(1+x)]^{1/2}$$

and a prime denotes $d/d\eta_1$.

Let us now examine the efflux from the boundary layer as implied by this solution. As $y_1 \rightarrow \infty$, $V_1 \rightarrow \beta_1 [2(1+x)]^{1/2}$, where $\beta_1 = 1.21678\dots$ from Van Dyke (1964), so that in order-one variables

$$v \rightarrow \epsilon^4 [Hdf/dx + \frac{1}{2}\beta_1(1+x)^{-1/2}].$$

When $H \ll 1$ and x is $O(1)$ this efflux is the usual boundary-layer one (implying a displacement thickness $\beta_1 \epsilon^4 [2(1+x)]^{1/2}$) plus an $O(H\epsilon^4)$ term, these being used to compute the second approximation in the external flow and thence the second-order boundary-layer flow. So the assumption of no $O(H)$ disturbance in the main stream and no first-order pressure effect in the boundary layer is valid for such x , justifying (7.5).

However, when we take $H \sim \epsilon$ and consider $x \sim \epsilon^3$, the efflux is of order ϵ^2 since $f(x)$ is order unity. A pressure variation of $O(\epsilon^2)$ is then fed back into the boundary layer and we observe that when $y \sim H = O(\epsilon)$ neglect of this ϵ^2 pressure effect is invalid, since dp/dx and $u \partial u / \partial x$ are both of $O(\epsilon^{-1})$. Overall, this indicates that a three-tiered structure is developing near $x = 0$: an outer region whose appearance is forced by the outflow from the main boundary layer; a middle region of thickness $\sim LRe^{-1/2}$ where pressure effects remain absent; and a viscous inner region where the pressure variation induced by the feedback properties of the outer region now has a first-order effect. The scalings, orders of magnitude and flow characteristics evolving here are exactly those of the systematic

rational expansions and matched solutions of the triple-deck structure and, as shown in §§ 2–5, the structure is able to cope with the non-uniformity appearing in the boundary-layer-theory approach above. For a fuller account of the necessity and importance of taking this $Re^{-\frac{3}{2}}$ scaling in x^*/L , we refer to Messiter (1970), who considers the allied problem of the flow in the wake of a flat plate. Limits other than $x \sim \epsilon^3$ and $H \sim \epsilon$ then provide only second-order corrections to the triple-deck solutions.

By letting the length of the hump tend to $O(L\epsilon^3)$ we see that a triple-deck analysis is required for all humps of length $L\epsilon^3$ or greater, the flow outside this region for the latter case being a small viscous perturbation of the Blasius solution without pressure effects. If the hump has length $L\epsilon^3$ or less, then the above argument shows that the flow in the triple deck must revert to the undisturbed boundary-layer form as $X \rightarrow \infty$ provided that separation, if it occurs, is only of the type producing a stagnant bubble near the hump. This is consistent with the supersonic and subsonic large- X solutions both for the point disturbance considered in §§ 4 and 5 and for a hump of dimensional length $2\lambda L\epsilon^3$, where λ is finite. In the latter problem, by use of the convolution integrals for $P(X)$ and $\tau(X)$, the same large- X solutions clearly hold apart from the inclusion of a factor

$$\int_{-\lambda}^{\lambda} F(X) dX$$

throughout.

8. Discussion

The different types of fluid motion corresponding to the various sizes of hump considered now seem to fit into a complete and consistent picture for both supersonic and subsonic main streams. For very small humps of dimensions $LRe^{-\frac{3}{2}}$ by $LRe^{-\frac{3}{2}}$, the full viscous Navier–Stokes equations apply with a pressure force dependent upon $y^*/L\epsilon^6$ as well as $x^*/L\epsilon^6$ (see appendix). For *all* humps larger than this, but not of full boundary-layer height, a triple-deck structure incorporating viscous effects and the induced pressure $P(X)$ describes the wake flow locally near $x^* = 0$ and the main perturbation effects act on the ϵ^3 scale in x^*/L . The match between the wake solutions on the $L\epsilon^3$ length scale and those on the $L\epsilon^6$ scale is direct, as is shown in the appendix, and even for the point disturbance discussed in § 4 the influence of the associated wake must be considered over a length $L\epsilon^3$. If the hump has length $\gg L\epsilon^3$, a triple-deck model still applies near $x^* = 0$, but for x^*/L of order unity the flow is a simple perturbation of the Blasius solution, without pressure gradient, as given in § 7. Thus the triple-deck results afford a continuous transition from the $LRe^{-\frac{3}{2}}$ problem for a size at one extreme to the problem considered in § 7 at the other extreme, and this is why so much significance has been placed on the flow features for the hump (1.3).

The solutions for the induced pressure $P(X)$ and skin friction $\tau(X)$ when the hump (1.3) has the parabolic profile $F(X) = X(1 - \theta X)/\theta$ for θX between 0 and 1, with $h \ll 1$, are presented in figure 3. Both P and τ are everywhere continuous but $\tau'(X)$ is discontinuous at each end of the obstacle, with $\tau'(0+)$ and $\tau'(\theta^{-1}+)$ infinite when $M_\infty < 1$, and $P'(X)$ experiences finite jumps there if $M_\infty < 1$. The

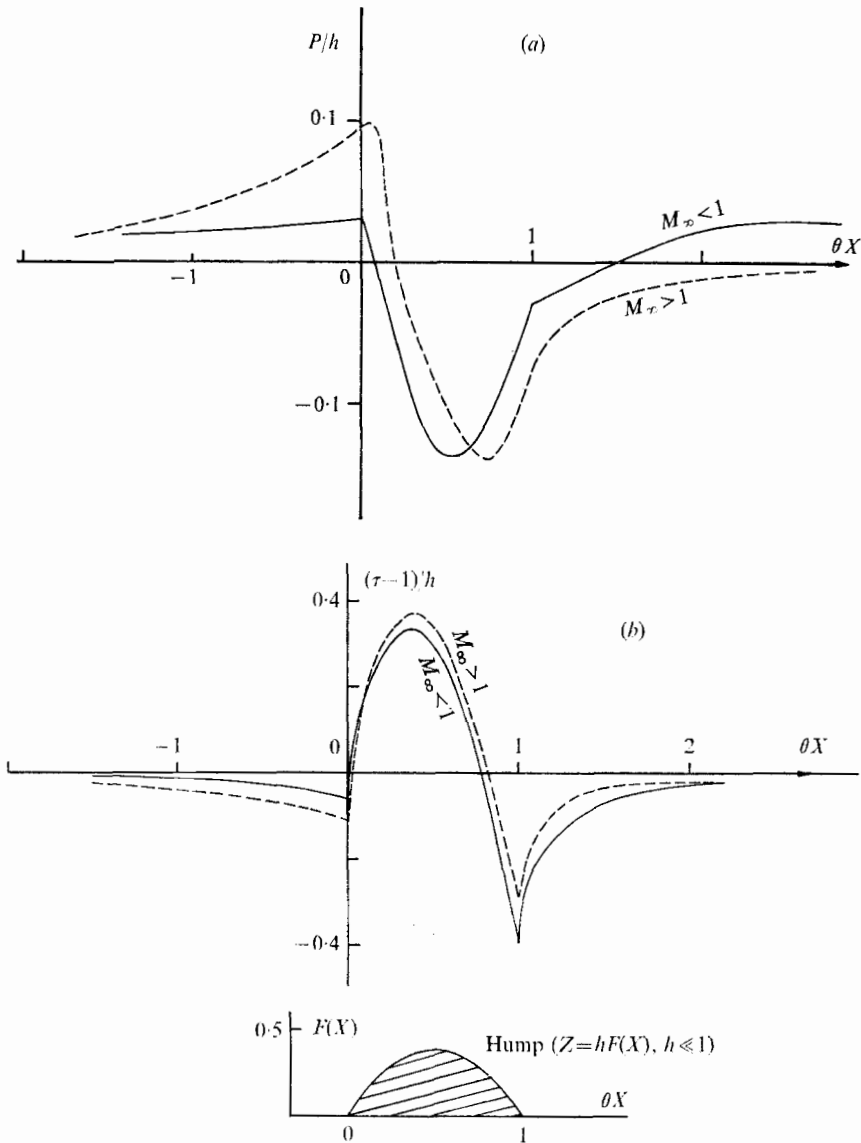


FIGURE 3. Distribution of (a) pressure $P(X)$ and (b) skin friction $\tau(X)$ for the flow past a parabolic hump for $M_\infty < 1$ and $M_\infty > 1$.

general development of the flow over the hump is physically sensible, although some further local treatment would obviously be desirable very near the end points to smooth out the irregularities there. It is observed that downstream of the hump the skin friction τ initially returns to its original value 1 from below despite the action of an adverse pressure gradient for some distance there. The most likely place for separation to occur first as the obstacle height h is increased to $O(1)$ would appear to be at the downstream end of the hump according to linearized theory but firm conclusions on this and other points of interest, particularly concerning the possibility of separation, must await a numerical treatment of the

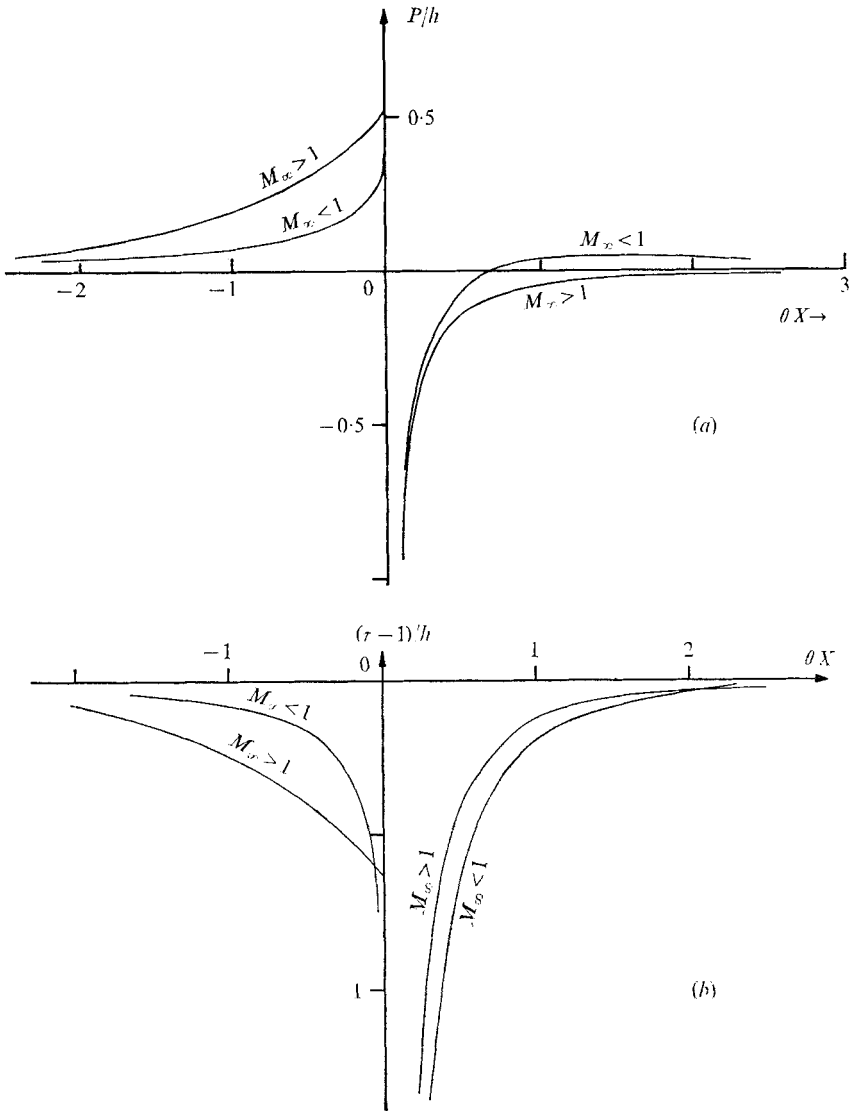


FIGURE 4. Graphs of (a) pressure P and (b) skin friction τ versus X for the point disturbance at the origin. The factor $h \ll 1$ is effectively a measurement of the body's cross-sectional area in the co-ordinates X and Z .

full nonlinear problem posed in §2. In figure 4 for $M_\infty \leq 1$ we show the variation of pressure and skin friction produced by the point disturbance within the lower deck. The precise details of the flow at the hump have been uncovered for (1.3) (see §3) and for (7.1) (see §7) but these details and the possibility of separation close to the obstacle have not yet been explored for the very small hump or for the Le^6 size. In terms of the flow right at the hump there may well be an intermediate regime of $O(Le^4)$ required to form the link between this last size and the triple deck size (1.3).

For the particular category (1.1) which lies within the range of applicability

of triple-deck theory, many of the flow features exhibited in the previous sections are similar in nature to those in Hunt's paper. However, in contrast to our results, the latter work produces an integral constant

$$I = \int_0^\infty z_1^2 \bar{u}_1 dz_1$$

(for notation see below), whereas we find the integral divergent, and predicts $C_2 \gg C_1$ in some circumstances. Since a number of other discrepancies can be revealed, some explanation and further comparison seem called for. The notation below is consistent with that of §§ 1–6. Interpreted in terms of asymptotic expansions involving the three most important parameters for the problem, namely Re , Δ and δ as defined in §1, Hunt's argument, erroneous in our view, starts in a region (I) $L\Delta$ by $L\Delta$. Here $u - y$, v and p are assumed to be of $O(\delta/\Delta^{\frac{2}{3}})$, $O(\delta/\Delta^{\frac{2}{3}})$ and $O(\delta\Delta^{\frac{1}{3}}/\epsilon^4)$ respectively. An inner region II then follows in which the corresponding orders of magnitude are

$$\delta/\epsilon^4, \quad \delta/\Delta^{\frac{2}{3}} \quad \text{and} \quad \delta\Delta^{\frac{1}{3}}/\epsilon^4, \quad \text{and} \quad X_1 = x^*/\Delta L \quad \text{and} \quad z_1 = y^*/\Delta^{\frac{1}{3}}\epsilon^4 L$$

are of $O(1)$. The resultant equations are then effectively (3.1)–(3.4) but the link, or interaction, with the main stream flow, represented by (3.5), is absent and the conditions $\bar{u}_1 \rightarrow 0$, $v \rightarrow -dp/dx$ as $z_1 \rightarrow \infty$ are used, where $\bar{u}_1 = (u - y)\epsilon^4/\delta$.

Now the skin-friction and pressure perturbations here agree in order of magnitude with those calculated in §4, but from (4.5) we see that triple-deck theory implies that the correct boundary condition as $y^*/L \rightarrow O(\epsilon^4)$ from below should be $u - y \rightarrow \epsilon hA(0) \sim \Delta\delta/\epsilon^7$ (and $\neq 0$) when $X \sim \lambda$. Thus the perturbation in u in region I should be much greater than that implied in the previous paragraph. The form (4.5) also shows that the non-dimensional efflux into the main boundary layer (from the lower deck) must have the form $\delta\Delta^{\frac{1}{3}}\epsilon^{-4}/yX_1^{-\frac{2}{3}}$. Our result is at variance, both in form and scaling, with the result (4.16) of Hunt. In our view it is the inconsistency in the assumption that the pressure in I and II is independent of main stream influence that causes the error in I; the fundamental link, which is represented by relations (2.9) and (2.10) between $A(X)$ and $P(X)$ and which still holds as $x^*/L \rightarrow O(\Delta)$ in the lower deck, has been missed. As shown in §4 and by the direct match discussed in the appendix even this very small hump produces in its wake effects that in terms of the interaction remain significant up to x^*/L of order ϵ^3 and hence for consistency the problem (1.1) must be considered on this length scale, i.e. by use of a triple-deck model.

The neglect of the main stream influence is not entirely justified and, although we agree with many of its basic assumptions, it is our opinion that Hunt's model is therefore not quite complete. Indeed, to have a first-order effect in any inner region the pressure must be of the induced (feedback) type, generated by the outflow from the boundary layer and hence bringing the influence of the main stream down to the inner regions of the boundary layer, close to the hump. The triple-deck structure and the flow features exhibited in the previous sections therefore override any purely local analysis for all humps lying outside the scope of the $L\epsilon^6$ by $L\epsilon^6$ regime.

We have shown that the forces and couple on a small hump are given by (6.2)–(6.5), and these results can be expected to hold for any point disturbance (such as (4.1)) defined by the limits (4.5). The two couples C_1 and C_2 , due to x -wise and Y -wise forces respectively, contribute equally to the highest order term of the total couple, C , which is directly proportional to the cross-sectional area and independent of the shape of the hump. From the discussions in §§4 and 5 we must conclude that overall there is no meaningful integral relation between C_1 , C_2 , F_1 or F_2 and the flow throughout the wake of the hump. The flow in the *near* wake, that is, for $X \ll 1$, may well exhibit a relation analogous to that found by Prandtl & Tietjens (1934) for flow in the wake of a body moving through a uniform flow field. A two-region structure within the lower deck, similar to those in Stewartson (1970*b*) and Smith (1972) and based on a Goldstein (1930) expansion scheme, seems likely to describe this near-wake motion. Such a structure would correspond to regions I and II above but with proper allowance made for the interaction (2.9) or (2.10); moreover, because the no-slip conditions on the hump surface have been satisfied by the triple-deck solutions, the indeterminacy inherent in the purely local approach is also resolved.

The wake far downstream ($X \gg 1$) of any small hump has the similarity form given in (4.10) and (4.11) for both subsonic and supersonic external flows. An interesting point of comparison here is that in the former regime the return of the motion to its far-upstream form takes place under a forcing pressure gradient $\sim X^{-3}$, whereas in the supersonic problem the pressure-gradient effect decays much more rapidly ($\sim X^{-\frac{3}{2}}$). Just aft of the very small hump – that is, in the *near* wake in terms of $X = (x^*/L) Re^{\frac{3}{2}}$ and the *far* wake in terms of the co-ordinate X_1 – the pressure $\sim X^{-\frac{3}{2}}$ and the skin-friction perturbation is negative and $\sim X^{-\frac{3}{2}}$, whilst

$$A(X) \sim -(h\theta/2\pi) (\frac{1}{2}3^{\frac{1}{2}}\pi - 3\Gamma(\frac{3}{2}) (\theta X)^{\frac{1}{2}} + \dots),$$

which implies that throughout the near wake the perturbation to the undisturbed boundary-layer solution for u^*/U_∞^* , caused by the introduction of the hump, is negative across the whole boundary layer. These near-wake results hold for $M_\infty \lesssim 1$, showing that the main stream retains its influence on the fluid motion even near the hump and that this influence is the same for a supersonic and a subsonic external flow.

My thanks and appreciation go to Professor K. Stewartson for directing my attention to this problem and for his subsequent interest in the present approach. I am also grateful to Professor M. J. Lighthill and the referee for their useful suggestions.

Appendix. The match with the solutions for very small humps of dimensions of $O(L Re^{-\frac{3}{2}})$ by $O(L Re^{-\frac{3}{2}})$

From the triple-deck results (4.4), (3.1) and (4.2) above, we can expect that when the hump's size is decreased so that its length and height are both of $O(L Re^{-\frac{3}{2}})$, just beyond the range permitted by (1.1), the X -wise and Z -wise velocities and the pressure perturbation near the hump ($X \sim \lambda$) are of orders

ϵ^2 , ϵ^2 and ϵ^4 respectively, bearing in mind the limiting process (4.5). Before this stage is reached, e.g. for all humps (1.1), the basic assumptions of the triple-deck structure remain appropriate. This may be seen in a number of ways; for instance the inviscid-displacement character of the main deck persists as the y variation in the pressure force p_2 , equation (SW 3.13), is effectively

$$\partial p_2 / \partial y = -\epsilon U_B(y) P'(X) \sim \Delta \delta \epsilon^{-7} X^{-\frac{3}{2}}$$

near the hump, under the limits (4.5), and as long as (1.1) holds this is always $\ll 1$. Also, the interaction is preserved as shown in §5. But for the $L\epsilon^6$ by $L\epsilon^6$ regime the triple-deck solutions finally break down as a comparison with Stewartson (1969) suggests and, putting $u = \epsilon^2 \hat{u} + o(\epsilon^2)$ and so on as implied above, the governing equations are found to be in fact the full Navier–Stokes equations (Stewartson 1968):

$$\partial(\psi, \nabla^2 \psi) / \partial(\hat{x}, \hat{y}) = -\nabla^4 \psi. \tag{A 1}$$

Here $(\hat{x}, \hat{y}) = (x/\epsilon^6, y/\epsilon^6)$, $\nabla^2 = \partial^2 / \partial \hat{x}^2 + \partial^2 / \partial \hat{y}^2$ and ψ is the stream function for the scaled velocity $(u/\epsilon^2, v/\epsilon^2)$. The boundary conditions are

$$\psi = \partial \psi / \partial \hat{y} = 0 \quad \text{on the hump} \quad \hat{y} = F(\hat{x}), \tag{A 2}$$

$$\psi \rightarrow \frac{1}{2} \hat{y}^2 \quad \text{as} \quad \hat{y} \rightarrow \infty, \tag{A 3}$$

the latter to provide the anticipated merging with the undisturbed boundary-layer solution far from the hump.

The remaining analysis is very similar to, but simpler than, that in Stewartson (1968) and so in referring to the paper we shall for convenience write only S. We apply the Oséén linearization procedure, replacing ψ in (A 1) by $\frac{1}{2} \hat{y}^2$ to obtain (S 2.9); x and y in S are of course equivalent to \hat{x} and \hat{y} in the present context. Linearizing (A 2), assuming $F(x)$ to be well-behaved and small, and applying Fourier transforms we obtain from (S 3.8)

$$\bar{F} = B(\omega) \int_0^\infty d\hat{y} e^{-\hat{y}|\omega|} \text{Ai}\{(\hat{y} - i\omega)(0 + i\omega)^{\frac{1}{2}}\}, \tag{A 4}$$

the notation being as defined in S. Our particular interest is in the behaviour at large \hat{x} downstream of the hump and so we examine the solutions for $\omega \rightarrow 0$, where ω is the transform variable. From (S 4.4) and (S 4.7), we then have in (A 4)

$$B(\omega) \sim 3\bar{F}(0)(0 + i\omega)^{\frac{1}{2}}. \tag{A 5}$$

Now, the linearized \hat{x} -momentum equation

$$\hat{y} \frac{\partial \hat{u}}{\partial \hat{x}} + \hat{v} = -\frac{\partial \hat{p}}{\partial \hat{x}} + \frac{\partial^2 \hat{u}}{\partial \hat{y}^2}$$

yields, at $\hat{y} = 0$, $d\{\hat{p}(\hat{x}, 0)\} / d\hat{x} = [\partial \chi / \partial \hat{y}]_{\hat{y}=0}$ for large \hat{x} , where $\chi = \nabla^2 \psi - 1$, so that using (S 3.4) and letting $w \rightarrow 0$ we obtain

$$\frac{d}{d\hat{x}} \{\hat{p}(\hat{x}, 0)\} \sim \frac{1}{2\pi} \int_{-\infty}^\infty 3\bar{F}(0)(0 + i\omega)^{\frac{1}{2}} \text{Ai}'(0) e^{i\omega \hat{x}} d\omega,$$

or
$$\frac{d}{d\hat{x}} \{\hat{p}(\hat{x}, 0)\} \sim \frac{3^{\frac{1}{2}}}{2\pi} \hat{x}^{-\frac{1}{2}} \Gamma(\frac{5}{3}) \bar{F}(0) \theta^{\frac{1}{2}} \quad \text{as} \quad \hat{x} \rightarrow \infty. \tag{A 6}$$

This matches exactly with the triple-deck solution (4.2) for the pressure gradient as $X \rightarrow 0$ there, taking into account all the scaling factors involved. Similar matching is found for the effective skin friction τ since here $\tau(\hat{x}) = 1 + \chi(\hat{x}, 0)$ gives

$$\tau \sim 1 + \frac{1}{2\pi} \int_{-\infty}^{\infty} 3\bar{F}(0) \text{Ai}(0) (0 + i\omega)^{\frac{1}{2}} e^{i\omega\hat{x}} d\omega \quad (\text{A } 7)$$

from (S 3.4) and (A 5), and solution (A 7) agrees with (4.3) for $X \rightarrow 0$.

The direct matching of the wake solutions for very small humps and those of the triple-deck type (1.3) is therefore demonstrated and a continuous transition from the one class of problems to the other as the hump size swells is indicated, without any need for an intermediate regime. This self-consistency further justifies our confidence in the picture presented at the beginning of §8.

REFERENCES

- GOLDSTEIN, S. 1930 *Proc. Camb. Phil. Soc.* **26**, 1.
 HUNT, J. C. R. 1971 *J. Fluid Mech.* **49**, 159.
 MESSITER, A. F. 1970 *SIAM J. Appl. Math.* **18**, 241.
 PRANDTL, L. & TIETJENS, O. 1934 *Applied Hydro and Aero Mechanics*. Dover.
 SMITH, F. T. 1972 D. Phil. dissertation, Oxford University.
 SMITH, F. T. & STEWARTSON, K. 1973 *Proc. Roy. Soc. A* (to appear).
 STEWARTSON, K. 1968 *Proc. Roy. Soc. A* **306**, 275.
 STEWARTSON, K. 1969 *Mathematika*, **16**, 106.
 STEWARTSON, K. 1970a *Quart. J. Mech. Appl. Math.* **23**, 137.
 STEWARTSON, K. 1970b *Proc. Roy. Soc. A* **319**, 289.
 STEWARTSON, K. 1971 *Quart. J. Mech. Appl. Math.* **24**, 387.
 STEWARTSON, K. & WILLIAMS, P. G. 1969 *Proc. Roy. Soc. A* **312**, 181.
 VAN DYKE, M. D. 1964 *Perturbation Methods in Fluid Mechanics*. Academic.